Optical Engineering

OpticalEngineering.SPIEDigitalLibrary.org

# Role of aberrations in the relative illumination of a lens system

Dmitry Reshidko
Jose Sasian

SPIE.

Dmitry Reshidko, Jose Sasian, "Role of aberrations in the relative illumination of a lens system," *Opt. Eng.* **55**(11), 115105 (2016), doi: 10.1117/1.OE.55.11.115105.

Optical Engineering 55(11), 115105 (November 2016)

# Role of aberrations in the relative illumination of a lens system

**Dmitry Reshidko*** **and Jose Sasian**
University of Arizona, College of Optical Sciences, 1630 East University Boulevard, Tucson, Arizona 85721, United States

**Abstract.** Several factors impact the light irradiance and relative illumination produced by a lens system at its image plane. In addition to cosine-fourth-power radiometric law, image and pupil aberrations and light vignetting also count. We use an irradiance transport equation to derive a closed form solution that provides insight into how individual aberration terms affect the light irradiance and relative illumination. The theoretical results are in agreement with real ray tracing.  [DOI: 10.1117/1.OE.55.11.115105]

Keywords: relative illumination; irradiance transport; aberration theory; lens design.

Paper 161432 received Sep. 13, 2016; accepted for publication Nov. 2, 2016; published online Nov. 29, 2016.

## 1 Introduction

The distribution of light at the focal plane of an optical system is an important aspect of a lens performance. Petzval[1] was well aware of the image plane illumination and back in 1858 stated, "A third quality of the new combination of lenses is the equal strength of light from the center to the utmost corners of a surface of the image." The term relative illumination was used as early as the 1900s, when photographers were concerned with the nonuniform illumination in different regions of the negative.[2,3] In the 1950s, the increasing demand for wide-angle lenses used for aerial photography and other purposes renewed interest in the subject. As shown in Fig. 1, it was found that the decrease in relative illumination of wide-angle lenses limited the angle of view of the early objectives to approximately 95 deg to 105 deg. The interest in creating accurate topographic maps led to the development of new lens design solutions capable of producing usable imagery over a greater angular field of view (FOV).[4]

Relative illumination is defined as the ratio of the irradiance on the focal plane at off-axis field positions to the irradiance at the center of the field. The relationship between the illumination and the field angle is derived from basic radiometric principles. For many practical purposes, the cosine-fourth-power ($\cos^4$)-law has been considered a reasonable approximation to the illumination fall-off produced by a lens at its focal plane; however, assumptions involved in the derivation of the $\cos^4$-law are often found to be incorrectly interpreted in the optical literature.[5]

The $\cos^4$-law states that the irradiance of different parts of the image formed by the optical system vary as the fourth power of the cosine of chief ray angle in object space. As some topographic lenses were found not to follow the $\cos^4$-law, the difference was referred to as the "lens effect."[4] Reiss showed that the $\cos^4$-law is precisely followed only by an optical system corrected for all image aberrations with an aperture stop that precedes the lens and the object at infinite distance.[6] Other authors have emphasized the importance of considering the effect of pupil aberrations and stop position on the illumination. It was found that it is possible to design a lens system in such a way that the decrease in illumination toward the edge of the field occurs more gradually than the $\cos^4$-law.[7–9]

Roossinov[10] patented a wide-angle lens that instead of the $\cos^4$-law realized a $\cos^3$-law. The area of the entrance aperture of this objective increases toward the edge of the FOV. This phenomenon is achieved by maximum divergence from Abbe's conditions of sines for the front half of the objective, with the object located in the plane of the diaphragm.

Rimmer outlined a method to accurately calculate relative illumination by real ray tracing. His method is based upon the theory developed by Hopkins and requires determining the size of the exit pupil in the direction cosine space.[11,12] Similar computation methods of relative illumination are used in modern lens design software.[13]

Although it is well known that the relative illumination in an optical system is a function of many variables, there is still confusion regarding the specific role of distortion, pupil aberrations, and aperture stop position on the distribution of light at the focal plane. In this paper, we use an irradiance transport equation to derive a closed form solution that approximates to fourth-order the image illumination fall-off and accounts for the illumination effects of aberrations in an unvignetted optical system. The role of individual aberration terms on the irradiance distribution at the focal plane is discussed and the results are in agreement with real ray tracing.

This manuscript represents a revised, refined, and expanded version of the related proceedings paper that outlines our research on the relative illumination in optical systems.[14]

## 2 Radiative Transfer in an Optical System

In this section, we review the radiometry of an optical system. Figure 2 illustrates the basic elements of an axially symmetric optical system and the geometry defining the transfer of radiant energy. Rays from a differential area d$A$ in object plane pass through the optical system and converge at the

*Address all correspondence to: Dmitry Reshidko, E-mail: dmitry@optics.arizona.edu

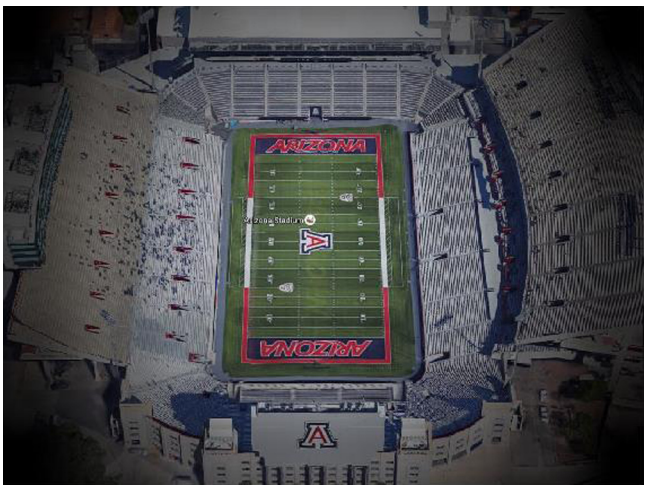


**Fig. 1** Stadium at the University of Arizona simulated through an early wide-angle lens (US 2031792). A sharp decrease in illumination toward the corners of the image limits the field-of-view of the objective.

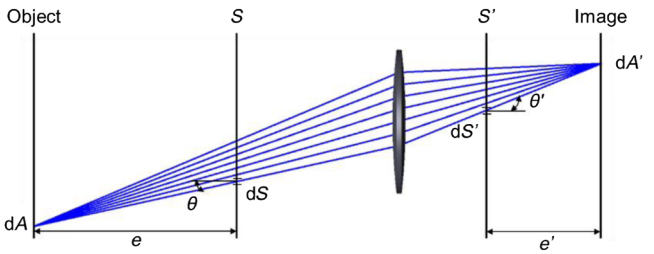


**Fig. 2** Geometry defining the transfer of radiant energy from differential area d$A$ in object space to the conjugate area d$A'$ in image space. The radiant flux through all cross sections of the beam is the same.

conjugate area d$A'$ in the image plane. We define an arbitrary plane $S$ in object space and a plane $S'$ conjugate to $S$ in image space. Differential cross sections of the beam d$S$ in $S$ and d$S'$ in $S'$ are conjugate.

In a lossless and passive optical system, the element of radiant flux d$\Phi$ is conserved through all cross sections of the beam. If we choose planes $S$ and $S'$ at the entrance and exit pupils, respectively, the radiative transfer equation becomes

$$\mathrm{d}\Phi_{o\to\mathrm{EP}} = \frac{L_o}{n_o^2}\frac{\mathrm{d}A\mathrm{d}S\cos^4(\theta)}{e^2} = \frac{L_o}{n_o^2}\frac{\mathrm{d}A'\mathrm{d}S'\cos^4(\theta')}{e'^2} = \mathrm{d}\Phi_{\mathrm{XP}\to i}, \tag{1}$$

where $L_o$ is the source radiance and $n_o$ is the index of refraction in object space. We assume that the source is Lambertian and, consequently, $L_o$ is constant. The object space angle $\theta$ is formed between the ray connecting d$A$ and d$S$, and the optical axis of the lens. Similarly, $\theta'$ is the image space angle between the ray connecting d$A'$ and d$S'$, and the optical axis. $e$ ($e'$) is the axial distance between the object (image) plane and the entrance (exit) pupil plane, respectively.

The irradiance is obtained by dividing the radiant flux that is incident on a surface by the unit area. It follows that

$$\mathrm{d}E = \frac{\mathrm{d}\Phi_{o\to\mathrm{EP}}}{\mathrm{d}A} = \frac{L_o}{n_o^2}\frac{\mathrm{d}S}{e^2}\cos^4(\theta), \tag{2}$$

and

$$\mathrm{d}E' = \frac{\mathrm{d}\Phi_{\mathrm{XP}\to i}}{\mathrm{d}A'} = \frac{L_o}{n_o^2}\frac{\mathrm{d}S'}{e'^2}\cos^4(\theta'), \tag{3}$$

where d$E$ is the differential of irradiance in the object plane and d$E'$ is the differential of irradiance at the conjugate point in the image plane. If an optical system is corrected for all image aberrations, then the irradiance at the object and image planes is related by the first-order transverse magnification $m$,

$$\mathrm{d}E' = \frac{\mathrm{d}E}{m^2}. \tag{4}$$

For an optical system with the finite aperture, the irradiance at any point is obtained by integrating Eq. (2) or Eq. (3) over the area of the pupil as

$$E = \int_{\mathrm{EP}} \frac{\mathrm{d}\Phi_{o\to\mathrm{EP}}}{\mathrm{d}A} = \frac{L_0}{n_0^2 e^2}\int_{\mathrm{EP}} \mathrm{d}S\cos^4(\theta), \tag{5}$$

and

$$E' = \int_{\mathrm{XP}} \frac{\mathrm{d}\Phi_{XP\to i}}{\mathrm{d}A'} = \frac{L_0}{n_0^2 e'^2}\int_{\mathrm{XP}} \mathrm{d}S'\cos^4(\theta'). \tag{6}$$

If no aberrations are present, the image space irradiance distribution may be evaluated using Eq. (4) as

$$E' = \frac{E}{m^2}. \tag{7}$$

Equations (5) and (6) are general and do not involve any approximations. However, care must be taken in evaluating these expressions, since the angles $\theta$ and $\theta'$ are functions of the field and pupil coordinates and may vary due to aberrations. In addition, the boundary of the area over which the integration is extended may also vary for different points in the field of the lens.

## 3 Irradiance Function

In this section, we define the irradiance function $E'(\vec{H},\vec{\rho})$ and show how aberrations are related to the irradiance distribution at the focal plane of an optical system. The irradiance function gives the relative irradiance of the beam at the image plane as a function of the normalized field $\vec{H}$ and aperture $\vec{\rho}$ vectors. The field vector lies in the object plane and the aperture vector may be defined in either entrance or exit pupil planes. Two vectors uniquely specify any ray propagating in the lens system. For an axially symmetrical optical system, in analogy with the aberration function, the irradiance function can be expressed as a polynomial.[15] In the limit of small aperture and to the fourth-order of approximation, the irradiance function is

$$E'(\vec{H},\vec{\rho}) = E'_{000} + E'_{200}(\vec{H}\cdot\vec{H}) + E'_{400}(\vec{H}\cdot\vec{H})^2. \tag{8}$$

This derivation implies that the irradiance is greater than zero for any point defined by the normalized field $\vec{H}$ and aperture $\vec{\rho}$ vectors.

### 3.1 *Thin Ideal Lens with the Stop Aperture at the Lens*

If the aperture stop is located at a thin ideal (no aberrations) lens, then both entrance and exit pupils coincide at the lens. The differential areas $dS$ and $dS'$ are equal and constant by construction. A point in the object plane defined by the field vector $\vec{H}$ is imaged ideally into a point in the image plane also defined by $\vec{H}$ as shown in Fig. 3.

In the limit of a small aperture, the variation of irradiance across the image plane is given by Eq. (3). We consider the irradiance contribution of the on-axis differential area at the stop to the image point defined by the field vector $\vec{H}$ and express the cosine as a function of the field vector. We use a Taylor series expansion to show that to the fourth-order of approximation the cosine-to-the-fourth-power of the angle between the ray connecting these two points and the optical axis is given by

$$\cos^4(\theta') = [1 - 2 \cdot \bar{u}'^2(\vec{H} \cdot \vec{H}) + 3 \cdot \bar{u}'^4(\vec{H} \cdot \vec{H})^2], \tag{9}$$

where $\bar{u}'$ is the chief ray slope in image space (see Appendix A). We substitute Eq. (9) into Eq. (3) and write the irradiance at the image plane of the ideal lens with the stop at the lens as

$$I'_{0/\text{ideal}} \equiv \frac{L_o}{n_o^2} \frac{dS'}{e'^2}, \tag{10}$$

and

$$E'_{\text{ideal}}(\vec{H}) = I'_{0/\text{ideal}} \cdot [1 - 2 \cdot \bar{u}'^2(H \cdot H) + 3 \cdot \bar{u}'^4(H \cdot H)^2], \tag{11}$$

where $I'_{0/\text{ideal}}$ is the irradiance value for the on-axis field point. We divide Eq. (11) by Eq. (10) to obtain the relative illumination as

$$Ri_{\text{ideal}}(\vec{H}) = 1 - 2 \cdot \bar{u}'^2(\vec{H} \cdot \vec{H}) + 3 \cdot \bar{u}'^4(\vec{H} \cdot \vec{H})^2. \tag{12}$$

Equation (12) is equivalent to the fourth-order expansion of the $\cos^4$-law in terms of first-order quantities. The irradiance at the image plane can also be computed by substituting Eq. (2) into Eq. (4) and evaluating the cosine function in object space. In the simple case of an ideal lens with the stop at the lens, the chief ray slopes in image and object spaces are equal: $\bar{u} = \bar{u}'$. Then, we can recover Eq. (12) by starting the calculation in either object or image space.

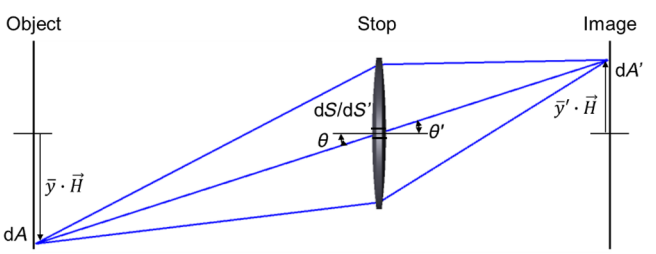


**Fig. 3** Geometrical variables involved in computing irradiance at the focal plane of a thin ideal, aberration free lens with the stop at the lens.

### 3.2 *Stop Aperture Follows the Lens*

If the aperture stop of the system follows the lens, then the exit pupil is the actual physical diaphragm. By construction, beams at the XP are uniform given that we choose to define rays at the exit pupil. For this example, it is easier to integrate Eq. (6) because of the simple limits of integration or use Eq. (3) in the limit of a small aperture.

By contrast to the previous case, in an actual system, rays may not pass through the ideal image point due to aberrations as shown in Fig. 4. The ray intersection with the image plane is determined by considering the transverse ray errors $\Delta\vec{H}$ and it is defined by the vector $\vec{H} + \Delta\vec{H}$.

In the presence of image aberrations, Eq. (6) determines the irradiance function $E'(\vec{H} + \Delta\vec{H}, \vec{\rho})$ at point $\vec{H} + \Delta\vec{H}$ of the image and coordinate $\vec{\rho}$ at the exit pupil. We write the differential of irradiance at the image as

$$E'(\vec{H} + \Delta\vec{H}, \vec{\rho}) \approx E'(\vec{H}, \vec{\rho}) + \nabla_H E'(\vec{H}, \vec{\rho}) \cdot \Delta\vec{H}, \tag{13}$$

where $\nabla_H E'(\vec{H}, \vec{\rho})$ is the gradient of the irradiance function with respect to the field vector $\vec{H}$. With no second-order terms in the aberrations function, the terms $\nabla_H E'(\vec{H}, \vec{\rho}) \cdot \Delta\vec{H}$ result in irradiance terms that are at least of fourth-order. In the limit of a small aperture for a system with distortion, the transverse ray errors to the third-order become

$$\Delta\vec{H} = -\frac{1}{Ж} W_{311}(\vec{H} \cdot \vec{H})\vec{H}. \tag{14}$$

By combining Eqs. (11), (13), and (14), and evaluating at the limit of small aperture (see Appendix B), the relative illumination of the lens system with the stop that follows the lens is

$$\begin{aligned} Ri_{\text{XP}}(\vec{H}) &= 1 - 2 \cdot \bar{u}'^2(\vec{H} \cdot \vec{H}) + \left[3 \cdot \bar{u}'^4 + \frac{4}{Ж} W_{311} \cdot \bar{u}'^2\right](\vec{H} \cdot \vec{H})^2 \\ &= Ri_{\text{ideal}} + \frac{4}{Ж} W_{311} \cdot \bar{u}'^2(\vec{H} \cdot \vec{H})^2. \end{aligned} \tag{15}$$

Thus, we conclude that the second-order relative illumination term is not affected by image distortion aberration $W_{311}$. The third-order distortion contributes to the fourth-order relative illumination coefficient. When negative "barrel" distortion is present, the irradiance over the field is more uniform than when the distortion is absent.

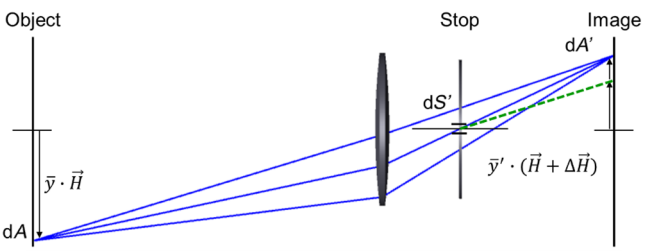


**Fig. 4** Geometrical variables involved in computing irradiance at the focal plane of the optical system with the aperture stop that follows the lens. Real rays (solid lines) and first-order rays (dashed lines) coincide at the exit pupil. Real rays may not pass through the ideal image point due to aberrations.

### 3.3 *Stop Aperture Precedes the Lens*

For this case, the entrance pupil is the actual physical diaphragm in the optical system. In the limit of small aperture, with the aperture vector $\vec{\rho}$ set at the entrance pupil and no image aberrations, Eqs. (2) and (4) determine the irradiance distribution at the focal plane. The expression for the relative illumination will be similar to Eq. (8), except the object space ray slopes are substituted with image space ray slopes

$$Ri_{\mathrm{EP}}(\vec{H}) = 1 - 2\cdot\bar{u}^2(\vec{H}\cdot\vec{H}) + 3\cdot\bar{u}^4(\vec{H}\cdot\vec{H})^2. \tag{16}$$

For the system with aberrations, on the other hand, we must use Eq. (3). The exit pupil now is a distorted image of the entrance pupil and the ray angle in Eq. (3) is determined by considering the transverse ray errors at both the image and exit pupil planes as shown in Fig. 5.

The irradiance function $E'(\vec{H}+\Delta\vec{H},\vec{\rho}+\Delta\vec{\rho})$ is evaluated at the image point defined by the vector $\vec{H}+\Delta\vec{H}$ and the coordinate at the exit pupil defined by the vector $\vec{\rho}+\Delta\vec{\rho}$. We can write for the differential of irradiance at the image plane as

$$E'(\vec{H}+\Delta\vec{H},\vec{\rho}+\Delta\vec{\rho}) \approx E'(\vec{H},\vec{\rho}) + \nabla_H E'(\vec{H},\vec{\rho}) \cdot \Delta\vec{H} + \nabla_\rho E'(\vec{H},\vec{\rho})\cdot\Delta\vec{\rho}, \tag{17}$$

where $\nabla_H E'(\vec{H},\vec{\rho})$ and $\nabla_\rho E'(\vec{H},\vec{\rho})$ are the gradients of the irradiance function with respect to the field $\vec{H}$ and aperture $\vec{\rho}$ vectors, respectively.

Moreover, if the differential area $\mathrm{d}S'$ in Eq. (3) is an image of the differential area $\mathrm{d}S$, then the size of $\mathrm{d}S'$ may also vary over the exit pupil and over the field due to pupil aberrations. Two differential areas are related by the determinant of the Jacobian of the transformation

$$\mathrm{d}S' = J(\vec{H},\vec{\rho})\mathrm{d}S. \tag{18}$$

We substitute Eq. (18) into Eq. (3) to find

$$\mathrm{d}E'(\vec{H},\vec{\rho}) = \frac{L_0}{n_0^2 e'^2}\mathrm{d}S'\cos^4(\theta') = \frac{L_0\mathrm{d}S}{n_0^2 e'^2}\cdot J(\vec{H},\vec{\rho}) \cdot\cos^4(\theta') = I'_{0/\mathrm{EP}}\cdot J(\vec{H},\vec{\rho})\cdot\cos^4(\theta'), \tag{19}$$

where $I'_{0/\mathrm{EP}}$ is the irradiance value for the on axis field point.

To obtain the Jacobian determinant, we express the transverse pupil ray aberration vector $\Delta\vec{\rho}$ in orthogonal components along unit vectors $\vec{h}$ and $\vec{k}$ as

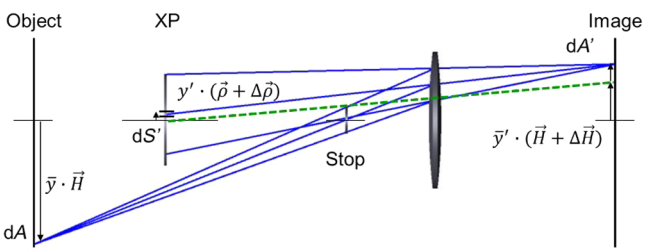


**Fig. 5** Geometrical variables involved in computing irradiance at the focal plane of the optical system with the aperture stop that precedes the lens. Real rays (solid lines) and first-order rays (dash lines) coincide at the entrance pupil. Real rays may not pass through the ideal point at both exit pupil and image planes due to aberrations.

$$\Delta\vec{\rho} = \Delta\rho_k\vec{k} + \Delta\rho_h\vec{h}, \tag{20}$$

where $\vec{h}$ is a unit vector along the field vector $\vec{H}$ and $\vec{k}$ is a unit vector perpendicular to the field vector $\vec{H}$. Then, we consider the transformations $\rho'_h = \rho_h + \Delta\rho_h$ and $\rho'_k = \rho_k + \Delta\rho_k$, which give the position of the given ray at the exit pupil, and so we find the Jacobian determinant

$$J(\vec{H},\vec{\rho}) = \frac{y'^2_{\mathrm{XP}}}{y^2_{\mathrm{EP}}}\left(1 + \nabla_\rho\Delta\vec{\rho} + \frac{\partial\Delta\vec{\rho}_h}{\partial\vec{\rho}_h}\frac{\partial\Delta\vec{\rho}_k}{\partial\vec{\rho}_k} - \frac{\partial\Delta\vec{\rho}_h}{\partial\vec{\rho}_k}\frac{\partial\Delta\vec{\rho}_k}{\partial\vec{\rho}_h}\right), \tag{21}$$

where $\nabla_\rho\Delta\vec{\rho}$ is the divergence of the transverse pupil ray error.[16,17] We substitute Eqs. (19) and (21) into Eq. (17), and neglecting six-order terms, the expression for the distribution of the irradiance at the focal plane becomes

$$E'(\vec{H}+\Delta\vec{H},\vec{\rho}+\Delta\vec{\rho}) \approx E'(\vec{H},\vec{\rho}) + \nabla_H E'(\vec{H},\vec{\rho}) \cdot \Delta\vec{H} + \nabla_\rho E'(\vec{H},\vec{\rho})\cdot\Delta\vec{\rho}\ldots + E'(\vec{H},\vec{\rho})\left[\nabla_\rho\Delta\vec{\rho} + \frac{\partial\Delta\vec{\rho}_h}{\partial\vec{\rho}_h}\frac{\partial\Delta\vec{\rho}_k}{\partial\vec{\rho}_k} - \frac{\partial\Delta\vec{\rho}_h}{\partial\vec{\rho}_k}\frac{\partial\Delta\vec{\rho}_k}{\partial\vec{\rho}_h}\right]. \tag{22}$$

With no second-order terms in the aberration function, the terms $\nabla_H E'(\vec{H},\vec{\rho})\cdot\Delta\vec{H}$ and $\nabla_\rho E'(\vec{H},\vec{\rho})\cdot\Delta\vec{\rho}$ result in irradiance terms that are at least of fourth-order. The terms $\left[\nabla_\rho\Delta\vec{\rho} + \frac{\partial\Delta\vec{\rho}_h}{\partial\vec{\rho}_h}\frac{\partial\Delta\vec{\rho}_k}{\partial\vec{\rho}_k} - \frac{\partial\Delta\vec{\rho}_h}{\partial\vec{\rho}_k}\frac{\partial\Delta\vec{\rho}_k}{\partial\vec{\rho}_h}\right]$ are at least of second-order and once multiplied by $E'(\vec{H},\vec{\rho})$ reveal second- and fourth-order terms. The relationships between pupil wavefront deformations and transverse pupil aberrations to fifth-order are given by Sasian.[18,19] In the limit of small aperture, only pupil spherical aberration and pupil coma contribute irradiance terms

$$\begin{aligned}\Delta\vec{\rho} =& \frac{4}{Ж}\overline{W}_{040}(\vec{H}\cdot\vec{H})\vec{H} + \frac{1}{Ж}\overline{W}_{131}[(\vec{H}\cdot\vec{H})\vec{\rho} + 2(\vec{H}\cdot\vec{\rho})\vec{H}]\ldots\\ &+\frac{1}{Ж}\overline{W}_{151}[(\vec{H}\cdot\vec{H})^2\vec{\rho} + 4(\vec{H}\cdot\vec{H})(\vec{H}\cdot\vec{\rho})\vec{H}]\ldots\\ &+\frac{1}{Ж}[5\cdot\overline{W}_{131}\cdot\bar{u}'^2 + 4\cdot\overline{W}_{040}\cdot\bar{u}'u'](\vec{H}\cdot\vec{H})^2\vec{\rho}\ldots\\ &-\frac{1}{Ж}[4\cdot\overline{W}_{131}\cdot\bar{u}'^2 + 8\cdot\overline{W}_{040}\cdot\bar{u}'u'](\vec{H}\cdot\vec{H})(\vec{H}\cdot\vec{\rho})\vec{H}\ldots\\ &-\frac{1}{Ж^2}[8\overline{W}_{040}W_{220} + 2\overline{W}_{131}W_{311}](\vec{H}\cdot\vec{H})^2\vec{\rho}\ldots\\ &-\frac{1}{Ж^2}[24\overline{W}_{040}W_{220} + 16\overline{W}_{040}W_{222} + 4\overline{W}_{131}W_{311}]\\ &\times(\vec{H}\cdot\vec{H})(\vec{H}\cdot\vec{\rho})\vec{H}.\end{aligned} \tag{23}$$

The fifth-order transverse pupil ray errors in Eq. (23) include extra terms that are products of fourth-order pupil aberration coefficients and the paraxial ray slopes $\bar{u}'$ and $u'$ in image space as well as terms that are products of the fourth-order image and pupil aberrations. By substituting Eqs. (14) and (23) into Eq. (22) and taking the required derivatives (see Appendix C), we find that in the limit of small aperture the relative illumination of the lens system with the stop that precedes the lens is

$$Ri_{EP}(\vec{H}) \approx 1 + \left[-2\bar{u}'^2 + \frac{4}{Ж}\bar{W}_{131}\right](\vec{H}\cdot\vec{H})\ldots + \left[3\bar{u}'^4 + \frac{4}{Ж}W_{311}\bar{u}'^2 + \frac{6}{Ж}\bar{W}_{151} - \frac{3}{Ж}\bar{W}_{131}\bar{u}'^2\right](\vec{H}\cdot\vec{H})^2\ldots - \frac{1}{Ж^2}[32\bar{W}_{040}W_{220} + 24\bar{W}_{040}W_{222} + 8\bar{W}_{131}W_{311}](\vec{H}\cdot\vec{H})^2\ldots + \frac{3}{Ж^2}\bar{W}_{131}\bar{W}_{131}(\vec{H}\cdot\vec{H})^2. \quad (24)$$

The residual field curvature and astigmatism of an objective lens that produces sharp imaging on a flat surface are small and additional terms that are products of these aberrations and pupil aberrations may be neglected. The fourth- and sixth-order pupil terms, $\bar{W}_{131}$ and $\bar{W}_{151}$, respectively, produce the aspect ratio change in the cross-section of the beam at the exit pupil as shown in Fig. 6.[20] By controlling pupil coma during the lens design process, it is possible to change the effective exit pupil area for off-axis field points and increase the amount of light accepted by the objective. This is known as the Slyusarev effect. In the presence of pupil spherical aberration $\bar{W}_{040}$, the beam at the exit pupil changes position laterally along different points in the field-of-view. However, it should be noted that when the stop precedes a lens and $W_{220} = W_{222} = 0$, spherical aberration of the pupil does not affect the relative illumination to fourth-order, though it may change the chief ray angle of incidence at the image plane.

The fourth-order pupil coma and image distortion are directly related

$$\bar{W}_{131} = W_{311} - \frac{Ж}{2}\Delta\{\bar{u}^2\}, \quad (25)$$

and to the second-order, the relative illumination in terms of object space slopes is

$$Ri_{EP}(\vec{H}) \approx 1 + \left[-2\bar{u}^2 + \frac{4}{Ж}W_{311}\right](\vec{H}\cdot\vec{H}). \quad (26)$$

The fourth-order expression for the relative illumination in terms of object space quantities is more complicated and does not provide additional insight. Finally, we compare Eq. (24) to Eq. (15) to show extra relative illumination terms that emerge from switching the aperture stop from the exit pupil to the entrance pupil. In the limit of small aperture and $W_{220} = W_{222} = 0$, the relative illumination becomes

$$Ri_{EP}(\vec{H}) \approx Ri_{XP}(\vec{H}) + \frac{4}{Ж}\bar{W}_{131}(\vec{H}\cdot\vec{H})\ldots + \left[\frac{6}{Ж}\bar{W}_{151} - \frac{3}{Ж}\bar{W}_{131}\bar{u}'^2 - \frac{8}{Ж^2}\bar{W}_{131}W_{311} + \frac{3}{Ж^2}\bar{W}_{131}\bar{W}_{131}\right](\vec{H}\cdot\vec{H})^2. \quad (27)$$

If the aperture stop precedes the lens, it is possible to have sufficient pupil aberrations such that the illumination will be more uniform or even constant over the entire field.

### 3.4 *Stop Aperture Between Components of the Lens*

In order to derive an expression for the image plane illumination of a lens system with an internal diaphragm, we divide the lens into two parts and evaluate the contribution of each part. As shown in Fig. 7, part A consists of all optical elements between the object plane and the diaphragm and thus has the aperture stop at the exit pupil. Part B includes all elements between the diaphragm and the image plane and has the aperture stop at the entrance pupil. By construction, the exit pupil of part A is the entrance pupil of part B. Furthermore, the image formed by A is the object of B.

If part A is corrected for all image aberrations, the beams after A converge to the image points defined by the field vector $\vec{H}$. The incoming beams incident on part B have no aberrations and in the limit of small aperture relative illumination of the system is given by the expression similar to Eq. (24)

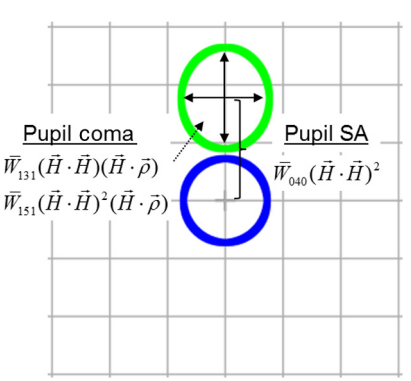


**Fig. 6** Beam footprints at the exit pupil in the presents of pupil aberrations for on-axis and off-axis field points. Pupil coma may change the area of the pupil, whereas pupil spherical aberration may shift the pupil transversely.

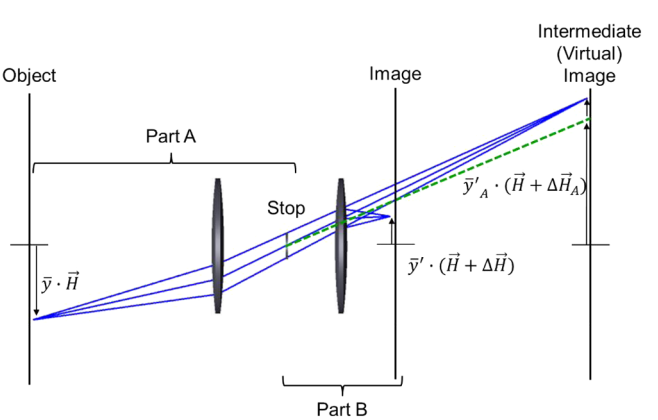


**Fig. 7** Geometrical variables involved in computing irradiance at the focal plane of the optical system with the aperture stop between components of the lens. The lens is divided into two parts A and B and contributions of each part are evaluated individually.

$$Ri_{\mathrm{EP}}(\vec{H}) \approx 1 + \left[-2\bar{u}'^2 + \frac{4}{\mathrm{Ж}}\bar{W}_{131B}\right](\vec{H}\cdot\vec{H})\ldots + \left[3\bar{u}'^4 + \frac{4}{\mathrm{Ж}}W_{311B}\bar{u}'^2 + \frac{6}{\mathrm{Ж}}\bar{W}_{151B} - \frac{3}{\mathrm{Ж}}\bar{W}_{131B}\bar{u}'^2\right](\vec{H}\cdot\vec{H})^2\ldots - \frac{1}{\mathrm{Ж}^2}[32\bar{W}_{040B}W_{220B} + 24\bar{W}_{040B}W_{222B} + 8\bar{W}_{131B}W_{311B}](\vec{H}\cdot\vec{H})^2\ldots + \frac{3}{\mathrm{Ж}^2}\bar{W}_{131B}\bar{W}_{131B}(\vec{H}\cdot\vec{H})^2, \quad (28)$$

where the subscript $B$ refers to aberration coefficients of part B alone. Most objectives with the internal diaphragm are designed to provide the best image quality only at the system focal plane. Parts A and B of the objective are not corrected individually. Part A forms a highly aberrated image, which is reimaged and compensated by the rest of the system. In the limit of small aperture, the distortion of A contributes transverse ray errors $\Delta\vec{H}_A$ to the third order given by

$$\Delta\vec{H}_A = -\frac{1}{\mathrm{Ж}}W_{311A}(\vec{H}\cdot\vec{H})\vec{H}. \quad (29)$$

The image points of A are now defined by the vector $\vec{H} + \Delta\vec{H}_A$ and the relative illumination of the system is calculated by evaluating Eq. (28) at $Ri_{\mathrm{EP}}(\vec{H} + \Delta\vec{H}_A)$. The second-order terms contribute extra fourth-order terms and the expression for the relative illumination of an optical system with internal diaphragm to fourth order is

$$Ri_{\mathrm{EP}}(\vec{H}) \approx 1 + \left[-2\bar{u}'^2 + \frac{4}{\mathrm{Ж}}\bar{W}_{131B}\right](\vec{H}\cdot\vec{H})\ldots + \left[3\bar{u}'^4 + \frac{4}{\mathrm{Ж}}W_{311A}\bar{u}'^2 + \frac{4}{\mathrm{Ж}}W_{311B}\bar{u}'^2 + \frac{6}{\mathrm{Ж}}\bar{W}_{151B} - \frac{3}{\mathrm{Ж}}\bar{W}_{131B}\bar{u}'^2\right](\vec{H}\cdot\vec{H})^2\ldots - \frac{1}{\mathrm{Ж}^2}[32\bar{W}_{040B}W_{220B} + 24\bar{W}_{040B}W_{222B} + 8\bar{W}_{131B}W_{311B}](\vec{H}\cdot\vec{H})^2\ldots + \left[\frac{3}{\mathrm{Ж}^2}\bar{W}_{131B}\bar{W}_{131B} - \frac{8}{\mathrm{Ж}^2}\bar{W}_{131B}W_{311A}\right](\vec{H}\cdot\vec{H})^2. \quad (30)$$

A comparison of Eqs. (28) and (30) reveals two additional terms that are caused by the aberrations of part A. The term $\frac{4}{\mathrm{Ж}}W_{311A}\bar{u}'^2$, combined with the term $\frac{4}{\mathrm{Ж}}W_{311B}\bar{u}'^2$, results in the total distortion of the system: $\frac{4}{\mathrm{Ж}}W_{311}\bar{u}'^2$. The term $-\frac{8}{\mathrm{Ж}^2}\bar{W}_{131B}W_{311A}$ is a product of the pupil aberration of part B and the image aberration of part A. In the special case of an optical system with symmetry around the stop, the distortion of parts A and B has the same magnitude but opposite sign. Moreover, each part of the symmetrical optical system is separately corrected for field curvature and astigmatism. We substitute $W_{311A} = -W_{311B}$ into Eq. (30) and write a simplified expression for the relative illumination of a symmetrical optical system

$$Ri_{\mathrm{EP}}(\vec{H}) \approx 1 + \left[-2\bar{u}'^2 + \frac{4}{\mathrm{Ж}}\bar{W}_{131B}\right](\vec{H}\cdot\vec{H})\ldots + \left[3\bar{u}'^4 + \frac{6}{\mathrm{Ж}}\bar{W}_{151B} - \frac{3}{\mathrm{Ж}}\bar{W}_{131B}\bar{u}'^2 + \frac{3}{\mathrm{Ж}^2}\bar{W}_{131B}\bar{W}_{131B}\right](\vec{H}\cdot\vec{H})^2. \quad (31)$$

We conclude that the relative illumination of a symmetrical optical system does not depend on the aberration contributions of elements that precede the diaphragm. More uniform illumination at the focal plane can be achieved by controlling the pupil coma of the rear part of the system.

### 3.5 *Summary of Relative Illumination Coefficients*

The second- and fourth-order relative illumination coefficients for different cases considered in Secs. 3.1–3.4 are summarized in Table 1.

### 3.6 *Relative Illumination Coefficient Verification*

In order to verify the derivation of the relative illumination coefficients, we determined their magnitude both analytically and numerically. A macro program was written to numerically calculate the coefficients by making an iterative fit to a selected set of relative illumination values across the FOV of an optical system. The iterative algorithm is similar to one used by Sasian to fit aberration coefficients.[16] The loop in Table 2 is executed.

The quantity $RELI(H)$ is the relative illumination at the specified field computed by real ray tracing in a lens design program. After a few iterations of this loop, the coefficients $E_{200}$ and $E_{400}$ converge to the theoretical values with insignificant error. This iterative fit methodology was used to test the coefficient values at several conjugate distances and aperture stop positions for both single surface and a system of several surfaces. The obvious agreement of the equations with the coefficients found with the above iterative loop supports the validity of the theory. For example, the relative illumination coefficients for a Landscape lens[21] shown in Fig. 8 were calculated both ways. We limit the FOV to 30 deg and close the diaphragm to meet a small aperture approximation. Table 3 presents a comparison of coefficients in which the differences in the eighth decimal place are likely due to the computational approach used.

## 4 Examples

In this section, we provide several examples of lenses that, rather than following the standard $\cos^4$-law, showed an improved illumination at the focal plane. Aberration theory is used to provide insight into the role of the individual aberration terms in the relative illumination of these lenses.

### 4.1 *Mobile Phone Camera Lens*

Miniature cameras for consumer electronics and mobile phones are rapidly growing technology. The system level requirements such as manufacturing cost, packaging, and sensor characteristics impose unique challenges for optical designers. The relative illumination is one of the interesting characteristics of miniature camera lens designs.

The typical distortion requirement in mobile camera lenses is <2% and the FOV is large (common FOV values

**Table 1** Summary of second- and fourth-order relative illumination coefficients for different cases. Relative illumination is expressed as a polynomial $Ri(\bar{H}) = 1 + Ri_{200}(\bar{H}\cdot\bar{H}) + Ri_{400}(\bar{H}\cdot\bar{H})^2$.

| Case | Second-order coefficient ($Ri_{200}$) | Fourth-order coefficient ($Ri_{400}$) |
|---|---|---|
| Thin ideal lens. Stop aperture at the lens | $-2\cdot\bar{u}'^2$ | $3\cdot\bar{u}'^4$ |
| Stop aperture follows the lens | $-2\cdot\bar{u}'^2$ | $3\cdot\bar{u}'^4 + \frac{4}{\bar{\kappa}}W_{311}\cdot\bar{u}'^2$ |
| Stop aperture precedes the lens | $-2\bar{u}'^2 + \frac{4}{\bar{\kappa}}\bar{W}_{131}$ | $3\bar{u}'^4 + \frac{4}{\bar{\kappa}}W_{311}\bar{u}'^2 + \frac{6}{\bar{\kappa}}\bar{W}_{151} - \frac{3}{\bar{\kappa}}\bar{W}_{131}\bar{u}'^2 + \frac{3}{\bar{\kappa}^2}\bar{W}_{131}\bar{W}_{131} - \frac{1}{\bar{\kappa}^2}[32\bar{W}_{040}W_{220} + 24\bar{W}_{040}W_{222} + 8\bar{W}_{131}W_{311}]$ |
| Stop aperture precedes the lens. $W_{220} = W_{222} = 0$ or $W_{220} = -\frac{24}{32}W_{222}$ | $-2\bar{u}'^2 + \frac{4}{\bar{\kappa}}\bar{W}_{131}$ | $3\bar{u}'^4 + \frac{4}{\bar{\kappa}}W_{311}\bar{u}'^2 + \frac{6}{\bar{\kappa}}\bar{W}_{151} - \frac{3}{\bar{\kappa}}\bar{W}_{131}\bar{u}'^2 - \frac{8}{\bar{\kappa}^2}\bar{W}_{131}W_{311} + \frac{3}{\bar{\kappa}^2}\bar{W}_{131}\bar{W}_{131}$ |
| Stop aperture between components of the lens | $-2\bar{u}^2 + \frac{4}{\bar{\kappa}}\bar{W}_{131B}$ | $3\bar{u}'^4 + \frac{4}{\bar{\kappa}}W_{311A}\bar{u}'^2 + \frac{4}{\bar{\kappa}}W_{311B}\bar{u}'^2 + \frac{6}{\bar{\kappa}}\bar{W}_{151B} - \frac{3}{\bar{\kappa}}\bar{W}_{131B}\bar{u}'^2 - \frac{1}{\bar{\kappa}^2}[32\bar{W}_{040B}W_{220B} + 24\bar{W}_{040B}W_{222B} + 8\bar{W}_{131B}W_{311B}] + \frac{3}{\bar{\kappa}^2}\bar{W}_{131B}\bar{W}_{131B} - \frac{8}{\bar{\kappa}^2}\bar{W}_{131B}W_{311A}$ |
| Symmetrical optical system | $-2\bar{u}'^2 + \frac{4}{\bar{\kappa}}\bar{W}_{131B}$ | $3\bar{u}'^4 + \frac{6}{\bar{\kappa}}\bar{W}_{151B} - \frac{3}{\bar{\kappa}}\bar{W}_{131B}\bar{u}'^2 + \frac{3}{\bar{\kappa}^2}\bar{W}_{131B}\bar{W}_{131B}$ |

are 65 deg to 75 deg). On the other hand, the chief ray incidence angle (CRA) on the sensor is usually limited to no more than 30 deg. The CRA impacts the relative illumination, which often is set to 50% at the sensor corners. For better CRA control, the aperture stop in a conventional mobile lens is placed close to the front, away from the image plane. The aperture stop position and the strong aspheric next to the image plane generate exit pupil spherical aberration, which reduces the CRA.

Mobile lenses are well-known for the extensive use of aspheric surfaces. The interaction of multiple aspherics within the design enables a high level of control over aberrations. Particularly, sharp imaging on a flat surface can be achieved without satisfying the classical requirement of having a Petzval sum nearly zero. The aspheric optical elements

**Table 2** Iterative algorithm that was used to fit relative illumination coefficients.

FOR $i = 1$ to 100

$H = 0.2$

$Ri = RELI(H)$

$E_{200} = (Ri - 1 - E_{400}H^4 - E_{600}H^6 - E_{800}H^8 - E_{1000}H^{10})\cdot H^{-2}$

$H = 0.4$

$Ri = RELI(H)$

$E_{400} = (Ri - 1 - E_{200}H^2 - E_{600}H^6 - E_{800}H^8 - E_{1000}H^{10})\cdot H^{-4}$

$H = 0.6$

$Ri = RELI(H)$

$E_{600} = (Ri - 1 - E_{200}H^2 - E_{400}H^4 - E_{800}H^8 - E_{1000}H^{10})\cdot H^{-6}$

$H = 0.8$

$Ri = \mathrm{RELI}(H)$

$E_{800} = (Ri - 1 - E_{200}H^2 - E_{400}H^4 - E_{600}H^6 - E_{1000}H^{10})\cdot H^{-8}$

$H = 1$

$Ri = RELI(H)$

$E_{1000} = (Ri - 1 - E_{200}H^2 - E_{400}H^4 - E_{600}H^6 - E_{800}H^8)\cdot H^{-10}$

NEXT

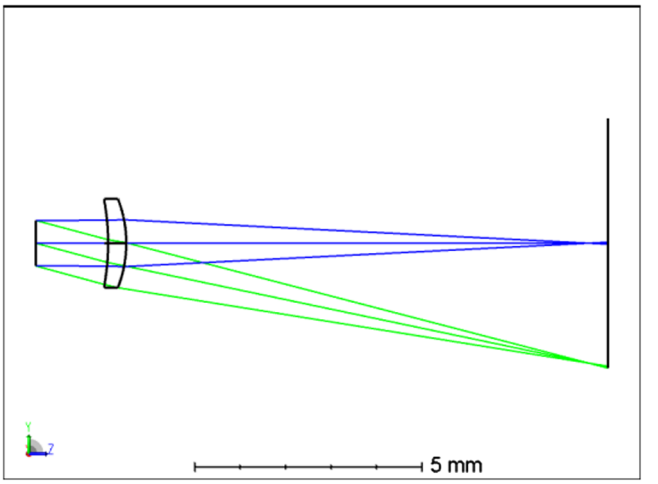


**Fig. 8** Landscape lens used to compare relative illumination coefficients computed analytically and numerically. In order to minimize fitting errors, the FOV of the lens is limited to 30 deg.

**Table 3** Comparison of relative illumination coefficients computed analytically and numerically. The agreement to eighth digits supports the correctness of the equations.

| Coefficient | Analytical equation | Numerical calculation |
|---|---|---|
| $E_{200}$ | −0.1014613598 | −0.1014613677 |
| $E_{400}$ | 0.0091763329 | 0.0091763317 |

located close to the image plane contribute higher-order field curvature and astigmatism. Different orders of the field curvature and astigmatism are balanced to compensate for any residual Petzval curvature.[22]

To illustrate how aberrations affect the relative illumination of a mobile camera lens, we evaluate different terms in Eq. (24) for one of the early miniature digital camera patents.[23] The three-element design shown in Fig. 9(a) covers a FOV of 64 deg at $f/2.8$. Field curvature and distortion plots are shown in Fig. 9(b). A small positive fourth-order distortion is compensated with a higher-order negative distortion resulting in <0.5% of total distortion. The Petzval radius is about two times the focal length; this clearly indicates that the residual field curvature is compensated by balancing higher orders of the field curvature and astigmatism. Aberration contributions to the relative illumination, sorted in descending order, are summarized in Table 4.

As expected, the major contribution to the deviation from the $\cos^4$-law comes from the pupil coma and distortion. However, since the distortion is small and pupil coma is proportional to the distortion, the ability to manipulate the relative illumination through these terms is limited. The products of residual field curvature, astigmatism, and pupil spherical aberration contribute significantly to the change in relative illumination of a mobile lens to fourth-order and may provide an effective degree of freedom during the lens design process. The relative illumination curves calculated with real ray tracing and using Eq. (24) are presented in Fig. 10. The plot shows excellent agreement between real ray tracing and the analytical solution over the entire FOV, confirming that our assumptions are still valid for relatively fast lenses with relatively large FOVs.

**Table 4** Contributions to the relative illumination according to Eq. (24) for U.S. 6441971.

| Second-order coefficient ($Ri_{200}$) | Numerical value | Fourth-order coefficient ($Ri_{400}$) | Numerical value |
|---|---|---|---|
| $-2\bar{u}'^2$ | −0.745977 | $3\bar{u}'^4$ | 0.417361 |
| $\frac{4}{\mathcal{K}}\bar{W}_{131}$ | 0.034043 | $\frac{6}{\mathcal{K}}\bar{W}_{151}$ | −0.055200 |
| | | $-\frac{24}{\mathcal{K}^2}\bar{W}_{040}W_{222}$ | 0.025298 |
| | | $\frac{4}{\mathcal{K}}W_{311}\bar{u}'^2$ | 0.018905 |
| | | $-\frac{32}{\mathcal{K}^2}\bar{W}_{040}W_{220}$ | −0.016739 |
| | | $-\frac{3}{\mathcal{K}}\bar{W}_{131}\bar{u}'^2$ | −0.009523 |
| | | $-\frac{8}{\mathcal{K}^2}\bar{W}_{131}W_{311}$ | 0.000863 |
| | | $\frac{3}{\mathcal{K}^2}\bar{W}_{131}\bar{W}_{131}$ | 0.000217 |
| Total | −0.711934 | | 0.343373 |

## 4.2 *Wide-Angle Lens*

The FOV of a wide-angle objective that follows the $\cos^4$-law is limited to approximately 95 deg to 105 deg due to a sharp decrease in illumination at the margin of the image. In U.S. Patent 2516724, shown in Fig. 11(a), the decrease in the illumination follows the $\cos^3$-law and this makes possible the widening of the angle of view up to 120 deg or more. In this design, the area of the entrance pupil increases toward the edge of the FOV approximately by the factor of two, and as the result, the area of oblique beams entering the objective differs negligibly from the area of the axial beams. The author explains this phenomenon by maximum divergence from Abbe's conditions of sines for the front half of the objective with an object located in the plane of the diaphragm, or in other words, by maximizing pupil coma for the front half of the objective as shown in Fig. 11(b).[10]

Aberration theory allows quantifying the required amount of pupil coma to achieve the $\cos^3$-law decrease in illumination. Similar to Eq. (9), we use Taylor series expansion to show that to the fourth order of approximation, the cosine-to-the-third-power of the angle in the object space is given by

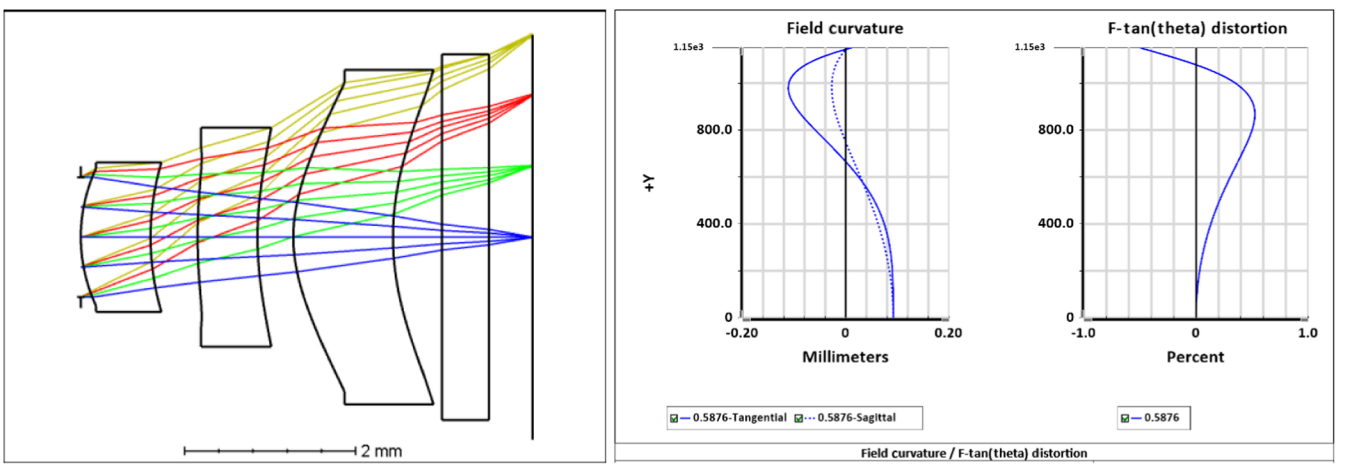


(a) (b)

**Fig. 9** U.S. Patent 6441971: (a) layout and (b) field curvature and distortion plot. Distortion correction requirements do not allow one to significantly reduce the chief ray incidence angle on the sensor (CRA). Exit pupil spherical aberration shifts the pupil radially and reduces the CRA. Higher order field curvature and astigmatism are balanced to compensate for the residual Petzval field curvature.

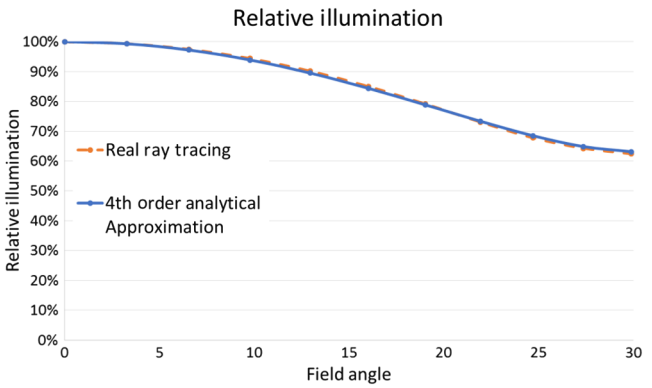


**Fig. 10** Relative illumination plot for U.S. Patent 6441971. Analytical equation and real ray tracing calculation show excellent agreement over the entire FOV.

$$\cos^3(\theta) \approx \left[1 - \frac{3}{2} \cdot \bar{u}^2(\vec{H} \cdot \vec{H}) + \frac{15}{8} \cdot \bar{u}^4(\vec{H} \cdot \vec{H})^2\right]. \tag{32}$$

U.S. Patent 2516724 consists of two more or less symmetrical halves. If we assume that two halves are exactly symmetrical, Eq. (31) can be used to predict relative illumination of this lens. In a symmetrical lens, the paraxial chief ray slope in object and image spaces are equal. The value of fourth- and six-order pupil coma are calculated by setting Eq. (31) equal to Eq. (32) and solving the following system of equations

$$\begin{aligned} &-2\bar{u}'^2 + \frac{4}{Ж}\bar{W}_{131B} = -\frac{3}{2}\bar{u}^2, \\ &3\bar{u}'^4 + \frac{6}{Ж}\bar{W}_{151B} - \frac{3}{Ж}\bar{W}_{131B}\bar{u}'^2 + \frac{3}{Ж^2}\bar{W}_{131B}\bar{W}_{131B} = \frac{15}{8}\bar{u}^4, \\ &\bar{u}' = \bar{u}. \end{aligned} \tag{33}$$

The term $\frac{3}{Ж^2}\bar{W}_{131B}\bar{W}_{131B}$ is small and can be neglected. We use the image pupil relationship in Eq. (25) and the fact that distortion in a symmetrical optical system is zero, to estimate the required amount of pupil coma to be

$$\bar{W}_{131B} = \frac{Ж}{8}\bar{u}^2, \tag{34}$$

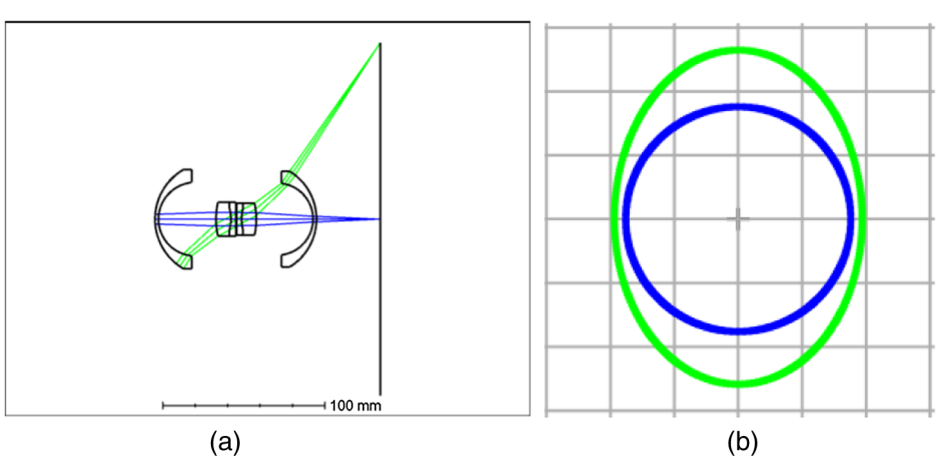


**Fig. 11** U.S. 2516724: (a) layout and (b) beam footprints at the exit pupil. The wide-angle objective consists of two nearly symmetrical halves. The form of the greatly curved exterior meniscus lens elements is of great importance. These meniscus lenses contribute substantial pupil coma, which increases the pupil area for oblique beams.

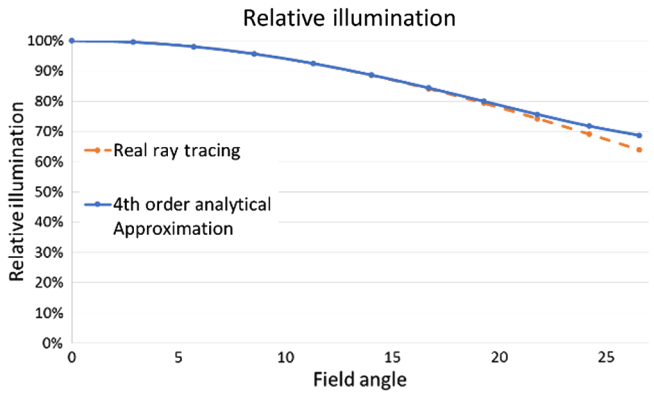


**Fig. 12** Relative illumination plot for U.S. Patent 2516724. Analytical fourth-order approximation and real ray tracing calculation show excellent agreement up to about 20 deg half field angle.

$$\bar{W}_{151B} = -\frac{Ж}{8}\bar{u}^4. \tag{35}$$

It is interesting to note that an objective lens that satisfies Eq. (34) also meets the Hershel condition for the object located in the plane of the pupil,[15] and therefore follows the decrease in the illumination according to the $\cos^3$-law to second order.

In Fig. 12, we show relative illumination curves calculated with real ray tracing alongside the analytical solution. Since the analytical solution provides a fourth-order approximation to relative illumination, there is excellent agreement with real ray tracing calculation only up to about 20 deg half field angle. For larger field angles, the six- and higher-order relative illumination terms, not presented here, contribute significantly to the illumination of the lens. The fourth-order approximation is not accurate enough to describe the relative illumination of the wide-angle lens in Fig. 12 beyond 20 deg half field angle.

### 4.3 *Optimization for a Target Relative Illumination*

The analytical solutions presented in this paper allow efficient optimization for a desired relative illumination during the lens design process. A straightforward way to calculate the relative illumination in a lens design program is to determine the exit pupil area by tracing the rays in reverse from

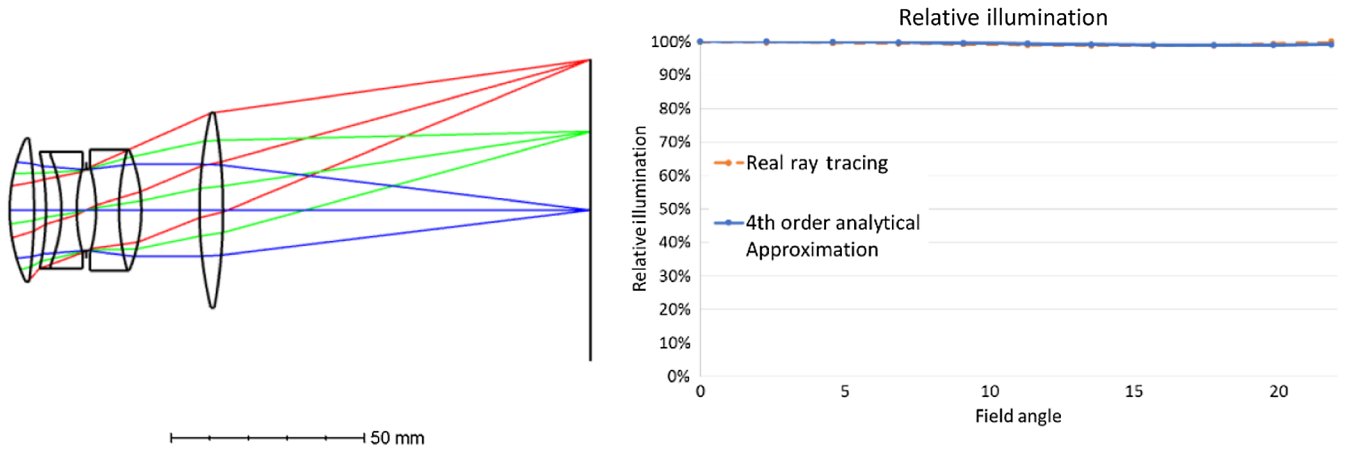


**Fig. 13** A double Gauss lens was reoptimized while targeting both second- and fourth-order relative illumination coefficients to zero. The fourth-order approximation is sufficiently accurate for practical purposes and allows efficiently optimizing for a desired relative illumination during the lens design process.

the image point in the direction cosines space. The relative illumination is proportional to the area of the pupil or to the number of rays that pass through the system.[12] Although this method is precise, the numerical integration requires tracing a large number of rays and therefore significantly slows down the optimization. On the other hand, we calculate the wave aberration coefficients by tracing only two first-order rays and estimate the relative illumination over the entire FOV of a lens.

We demonstrate that the fourth-order approximation to the relative illumination is sufficiently accurate for practical purposes and can be used, e.g., to design a lens that has uniform illumination over the field. The objective being modified is a double Gauss lens that operates at $f/4$ and has a FOV of 40 deg. We limit the distortion to be <5% and target both second- and fourth-order relative illumination coefficients to zero. The resulting system layout and relative illumination plot are shown in Fig. 13. The image is equally illuminated over its entire area.

## 5 Conclusion

Among other image quality requirements, the relative illumination may have a strong impact on the performance of a lens. A number of authors have shown that the standard $\cos^4$-law of illumination fall-off is not accurate for an objective with image and pupil aberrations. However, a detailed and comprehensive investigation of the relation between relative illumination and individual aberration coefficients to fourth-order has not been previously discussed.

In this paper, the problem has been approached from the aberration theory point of view. An irradiance transport equation provides the irradiance changes at the exit pupil of the optical system, given the irradiance at the entrance pupil and the pupil aberration function. We use this irradiance transport equation to derive a closed form solution that approximates the image illumination fall-off and accounts for the illumination effects of aberrations in an unvignetted optical system.

We consider three different possible aperture stop positions: as the last element, as the first element, and between components of the lens system. Only the piston irradiance term is considered in the derivation, which is equivalent to the specification of a small diaphragm. Equations (15), (24), and (30) give the relative illumination to the fourth-order of approximation in terms of aberration coefficients for each case, respectively. A macro program for calculating the image wave aberration coefficients to sixth-order is provided by Sasian.[24] The pupil wave aberration coefficients to six-order can be calculated using the same macro and exchanging roles of the marginal and chief rays.

If the aperture stop of the system follows the lens, only third-order distortion contributes to the fourth-order relative illumination coefficient. On the other hand, if the aperture stop precedes the lens, both image and pupil aberrations affect the relative illumination. In this case, it is possible to have sufficient pupil aberrations such that the illumination will be more uniform or even constant over the entire field. If the aperture stop is located between the components of the lens, we need to consider image and pupil aberration contributions of the rear half and distortion of the front half of the objective. This result reveals a new path to improve image quality and required illumination by balancing aberrations of the two halves.

In several special cases, it is possible to come up with a more compact, reduced form of the equations. Table 1 summarizes second- and fourth-order relative illumination coefficients for different cases. The results are validated with real ray tracing. The agreement to eighth digits of precision adds support the correctness of the equations.

Finally, we provide several examples of lenses that instead of the $\cos^4$-law show improved illumination at the focal plane. Aberration theory is used to provide insight into the role of individual aberration coefficients on the relative illumination of these lenses. Although the specification of a small diaphragm was used in the derivation, this approximation has shown to be sufficiently accurate for practical purposes.

Our future research on the irradiance transport in a lens system will involve derivation of other fourth-order irradiance coefficients in terms of wave aberration coefficients. If all fourth-order irradiance terms are considered, it will be possible to analytically calculate the relative illumination more accurately for a lens system with a finite aperture; however, we expect that the equations will become too complex to provide any additional intuitive insight.

## Appendix A: Series Expansion of the Cosine-to-the-Fourth-Power of the Ray Angle

By definition, the cosine-to-the-fourth-power of the angle between the ray connecting the point $(x'_{XP}, y'_{XP})$ in the exit pupil plane and point $(x'_i, y'_i)$ in the image plane, and the optical axis is

$$\cos^4(\theta') = \left\{\frac{e'}{[(x'_{XP}-x'_i)^2+(y'_{XP}-y'_i)^2+e'^2]^{1/2}}\right\}^4 = \left\{\frac{1}{\left[1+\frac{(x'_{XP}-x'_i)^2}{e'^2}+\frac{(y'_{XP}-y'_i)^2}{e'^2}\right]^{1/2}}\right\}^4 = \frac{1}{\left[1+\frac{(x'^2_{XP}+y'^2_{XP})}{e'^2}+\frac{(x'^2_i-y'^2_i)}{e'^2}-\frac{2\cdot(x'_{XP}x'_i-y'_{XP}y'_i)}{e'^2}\right]^2}, \quad (36)$$

where $e'$ is the axial distance between the image plane and the exit pupil plane. For an ideal (aberration free) lens with the stop aperture at the lens, points $(x'_{XP}, y'_{XP})$ and $(x'_i, y'_i)$ may be expressed in terms of the first-order system parameters as

$$(x'^2_i + y'^2_i)^{1/2} = \bar{y}' \cdot \vec{H} \quad (x'^2_{XP} + y'^2_{XP})^{1/2} = y' \cdot \vec{\rho}, \quad (37)$$

and

$$\bar{u}' = -\frac{\bar{y}'}{e'} \quad u' = \frac{y'}{e'}. \quad (38)$$

Here $\bar{y}'$ and $\bar{u}'$ are the chief ray height and slope at the image plane, $y'$ and $u'$ are the marginal ray height and slope at the exit pupil plane. We substitute Eqs. (37) and (38) into (36) and write first two terms of a Taylor series expression to obtain the fourth-order approximation to the cosine-to-the-fourth-power of the ray angle as

$$\begin{aligned}\cos^4(\theta') &= \frac{1}{[1+\bar{u}'^2(\vec{H}\cdot\vec{H})+u'^2(\vec{\rho}\cdot\vec{\rho})+2\cdot u'\bar{u}'(\vec{H}\cdot\vec{\rho})]^2}\\ &= 1-2\cdot[\bar{u}'^2(\vec{H}\cdot\vec{H})+u'^2(\vec{\rho}\cdot\vec{\rho})+2\cdot u'\bar{u}'(\vec{H}\cdot\vec{\rho})]\ldots\\ &\quad +3\cdot[\bar{u}'^2(\vec{H}\cdot\vec{H})+u'^2(\vec{\rho}\cdot\vec{\rho})+2\cdot u'\bar{u}'(\vec{H}\cdot\vec{\rho})]^2\\ &= 1-2\cdot\bar{u}'^2(\vec{H}\cdot\vec{H})-2\cdot u'^2(\vec{\rho}\cdot\vec{\rho})-4\cdot u'\bar{u}'(\vec{H}\cdot\vec{\rho})\ldots\\ &\quad +3\cdot\bar{u}'^4(\vec{H}\cdot\vec{H})^2+12\cdot u'^3\bar{u}'(\vec{H}\cdot\vec{\rho})(\vec{\rho}\cdot\vec{\rho})+12\\ &\quad \cdot u'^2\bar{u}'^2(\vec{H}\cdot\vec{\rho})^2+6\cdot u'^2\bar{u}'^2(\vec{H}\cdot\vec{H})(\vec{\rho}\cdot\vec{\rho})\ldots\\ &\quad +12\cdot u'\bar{u}'^3(\vec{H}\cdot\vec{H})(\vec{H}\cdot\vec{\rho})+3\cdot u'^4(\vec{\rho}\cdot\vec{\rho})^2. \end{aligned} \quad (39)$$

In the limit of small aperture $\vec{\rho}\to 0$, and Eq. (39) is reduced to a more simplified form give in Eq. (9).

## Appendix B: Irradiance Function of an Optical System with the Stop Aperture that Follows the Lens

To calculate the irradiance distribution at the focal plane of an optical system with the aperture stop that follows the lens, we evaluate the terms in Eq. (13). The first term $E'(\vec{H},\vec{\rho})$ is given by Eq. (11). To calculate the second term $\nabla_H E'(\vec{H},\vec{\rho})$ we take the gradient of the irradiance function given in Eq. (11) with the respect to the field vector $\vec{H}$. Thompson has shown that the gradient operator is given by the derivative of the function with respect to the designated vector.[25] It follows that to first-order

$$\nabla_H E'(\vec{H},\vec{\rho}) = I'_{0/\text{ideal}}\cdot[-4\cdot\bar{u}'^2\cdot\vec{H}], \quad (40)$$

and to fourth-order

$$\begin{aligned}\nabla_H E'(\vec{H},\vec{\rho})\cdot\Delta\vec{H} &= I'_{0/\text{ideal}}\\ &\quad\cdot[-4\cdot\bar{u}'^2\cdot\vec{H}]\times\left[-\frac{1}{Ж}W_{311}(\vec{H}\cdot\vec{H})\vec{H}\right] =\\ &= I'_{0/\text{ideal}}\cdot\frac{4}{Ж}\cdot\bar{u}'^2\cdot W_{311}(\vec{H}\cdot\vec{H})^2. \end{aligned} \quad (41)$$

Finally, the irradiance function in Eq. (13) is

$$\begin{aligned}E'(\vec{H}+\Delta\vec{H},\vec{\rho}) &\approx I'_{0/\text{ideal}}\\ &\quad\cdot[1-2\cdot\bar{u}'^2(\vec{H}\cdot\vec{H})+3\cdot\bar{u}'^4(\vec{H}\cdot\vec{H})^2]+I'_{0/\text{ideal}}\cdot\frac{4}{Ж}\\ &\quad\cdot\bar{u}'^2\cdot W_{311}(\vec{H}\cdot\vec{H})^2. \end{aligned} \quad (42)$$

## Appendix C: Irradiance Function of an Optical System with the Stop Aperture that Precedes the Lens

To calculate the irradiance distribution at the focal plane of an optical system with the aperture stop that precedes the lens, we evaluate the terms in Eq. (22). The first $E'(\vec{H},\vec{\rho})$ and second $\nabla_H E'(\vec{H},\vec{\rho})\cdot\Delta\vec{H}$ terms are given by Eqs. (11) and (41), respectively. To calculate the third term $\nabla_\rho E'(\vec{H},\vec{\rho})\cdot\Delta\vec{\rho}$, we take the gradient of the irradiance function with the respect to the field vector $\vec{\rho}$ and keep only first-order terms. With no second-order terms in the aberrations function and in the limit of small aperture $\vec{\rho}\to 0$, it follows that

$$\begin{aligned}\nabla_\rho E'(\vec{H},\vec{\rho})\cdot\Delta\vec{\rho} &= I'_{0/\text{EP}}\\ &\quad\cdot[-4\cdot u'\cdot\bar{u}'\cdot\vec{H}]\times\left[\frac{4}{Ж}\overline{W}_{040}(\vec{H}\cdot\vec{H})\vec{H}\right] =\\ &\quad -I'_{0/\text{EP}}\cdot\frac{16}{Ж}\cdot u'\cdot\bar{u}'\cdot\overline{W}_{040}(\vec{H}\cdot\vec{H})^2. \end{aligned} \quad (43)$$

Sasian has shown the procedure to calculate the divergence operator of the function with respect to the designated vector.[16,26] Following this procedure and taking the required derivatives, we find that in the limit of small aperture the fourth term in Eq. (22) is

$$\begin{aligned}E'(\vec{H},\vec{\rho})\cdot&\left[\nabla_\rho\Delta\vec{\rho}+\frac{\partial\Delta\vec{\rho}_h}{\partial\vec{\rho}_h}\frac{\partial\Delta\vec{\rho}_k}{\partial\vec{\rho}_k}-\frac{\partial\Delta\vec{\rho}_h}{\partial\vec{\rho}_k}\frac{\partial\Delta\vec{\rho}_k}{\partial\vec{\rho}_h}\right] =\\ &I'_{0/\text{EP}}\cdot[1-2\cdot\bar{u}'^2(\vec{H}\cdot\vec{H})]\times\left[\frac{4}{Ж}\bar{W}_{131}(\vec{H}\cdot\vec{H})\right.\\ &+\frac{6}{Ж}\bar{W}_{151}(\vec{H}\cdot\vec{H})^2\ldots\\ &+\frac{1}{Ж}[5\cdot\bar{W}_{131}\cdot\bar{u}'^2+16\cdot\bar{W}_{040}\cdot\bar{u}'u'](\vec{H}\cdot\vec{H})^2\ldots\\ &-\frac{1}{Ж^2}[32\bar{W}_{040}W_{220}+24\bar{W}_{040}W_{222}\\ &+8\bar{W}_{131}W_{311}](\vec{H}\cdot\vec{H})^2\ldots\\ &\left.+\frac{3}{Ж^2}\bar{W}_{131}\bar{W}_{131}(\vec{H}\cdot\vec{H})^2\right]. \end{aligned} \quad (44)$$

Finally, the irradiance function in Eq. (22) is obtained by combining Eqs. (11), (41), and (44) and keeping only second- and fourth-order terms as

$$
\begin{aligned}
E'(\vec{H}+\Delta\vec{H},\vec{\rho}+\Delta\vec{\rho}) &\simeq I'_{0/\mathrm{EP}} \\
&\cdot [1+\left[-2\bar{u}'^2+\frac{4}{Ж}\bar{W}_{131}\right](\vec{H}\cdot\vec{H})\ldots \\
&+\left[3\bar{u}'^4+\frac{4}{Ж}W_{311}\bar{u}'^2+\frac{6}{Ж}\bar{W}_{151}-\frac{3}{Ж}\bar{W}_{131}\bar{u}'^2\right](\vec{H}\cdot\vec{H})^2\ldots \\
&-\frac{1}{Ж^2}\left[32\bar{W}_{040}W_{220}+24\bar{W}_{040}W_{222}\right. \\
&\left.+8\bar{W}_{131}W_{311}](\vec{H}\cdot\vec{H})^2\ldots\right. \\
&\left.+\frac{3}{Ж^2}\bar{W}_{131}\bar{W}_{131}(\vec{H}\cdot\vec{H})^2\right]. \qquad (45)
\end{aligned}
$$

## References


1. J. Petzval, "Professor Petzval new lens," in *Photographic Notes*, S. Thomas, Ed., pp. 118–121, Photographic Society of Scotland, London (1858).
2. M. von Rohr, "Distribution of light on the focal plane of a photographic objective," *Zeitschr. Insttrymentenk.* **18**, 171–180 (1898).
3. T. R. Dallmeyer, "Technical meeting," *Photogr. J.* **19**, 221–232 (1895).
4. F. E. Washer, "Characteristics of wide-angle airplane camera lenses," *J. Res. Nat. Bureau Stand.* **29**, 233–246 (1942).
5. J. M. Palmer and B. G. Grant, *The Art of Radiometry*, Chapter 2, pp. 30–38, SPIE Press, Bellingham, Washington (2010).
6. M. Reiss, "The $\cos^4$ law of illumination," *J. Opt. Soc. Am.* **35**(4), 283–288 (1945).
7. M. Reiss, "Notes on the $\cos^4$ law of illumination," *J. Opt. Soc. Am.* **38**(11), 980–986 (1948).
8. I. C. Gardner, "Validity of the cosine-fourth-power law of illumination," *J. Res. Nat. Bur. Stand.* **39**, 213–219 (1947).
9. F. Wachendorf, "The condition of equal irradiance and the distribution of light in images formed by optical systems without artificial vignetting," *J. Opt. Soc. Am.* **43**(12), 1205–1208 (1953).
10. M. M. Roossinov, "Wide angle orthoscopic anastigmatic photographic objective," U.S. Patent No. 2516724 (1950).
11. H. H. Hopkins, "Canonical and real-space coordinates used in the theory of image formation," *Appl. Opt. Opt. Eng.* **9**, 8 (1983).
12. M. P. Rimmer, "Relative illumination calculations," *Proc. SPIE* **655**, 99–104 (1986).
13. Zemax LLC., *OpticStudio Manual*, Zemax LLC., USA (2016).
14. D. Reshidko and J. Sasian, "The role of aberrations in the relative illumination of a lens system," *Proc. SPIE* **9948**, 994806 (2016).
15. J. Sasian, *Introduction to Aberrations in Optical Imaging Systems*, Cambridge University Press, Chapter 13, pp. 173–186 (2013).
16. J. Sasian, "Theory of six-order wave aberrations," *Appl. Opt.* **49**(16), D69–D95 (2010).
17. C. Roddier and F. Roddier, "Wave-front reconstruction from defocused images and the testing of ground-based optical telescopes," *J. Opt. Soc. Am. A* **10**(11), 2277 (1993).
18. J. Sasian, *Introduction to Aberrations in Optical Imaging Systems*, Chapter 12, pp. 162–172, Cambridge University Press, New York (2013).
19. J. Sasian, *Introduction to Aberrations in Optical Imaging Systems*, Cambridge University Press, Chapter 14, pp. 187–204 (2013).
20. J. Sasian, "Interpretation of pupil aberrations in imaging systems," *Proc. SPIE* **6342**, 634208 (2006).
21. R. Kingslake, *Lens Design Fundamentals*, 2nd ed., Chapter 12, pp. 325–329, Academic Press (2010).
22. D. Reshidko and J. Sasian, "Optical analysis of miniature lenses with curved imaging surfaces," *Appl. Opt.* **54**(28), E216–E223 (2015).
23. I. Ning, "Compact lens with external aperture stop," U.S. Patent No. 6441971 B2 (1999).
24. J. Sasian, *Introduction to Aberrations in Optical Imaging Systems*, Cambridge University Press, pp. 247–257 (2013).
25. K. Thompson, "Description of the third-order optical aberrations of near-circular pupil optical systems without symmetry," *J. Opt. Soc. Am.* **22**, 1389–1401 (2005).
26. J. Sasian, "Theory of six-order wave aberrations: errata," *Appl. Opt.* **49**(33), 6502 (2010).



**Dmitry Reshidko** is a PhD candidate whose research involves development of imaging techniques and methods for image aberration correction, innovative optical design, fabrication, and testing of state-of-the-art optical systems.

**Jose Sasian** is a professor at the University of Arizona. His interests are in teaching optical sciences, optical design, illumination optics, optical fabrication and testing, telescope technology, optomechanics, lens design, light in gemstones, optics in art and art in optics, and light propagation. He is a fellow of SPIE and the Optical Society of America and is a lifetime member of the Optical Society of India.